Virtual states in electron-molecule scattering via modified effective-range theory

Kamil Fedus [*] and Grzegorz Karwasz [†]
Institute of Physics, Faculty of Physics, Astronomy and Informatics, Nicolaus Copernicus University, Grudziadzka 5/7, 87-100 Toruń, Poland

(Received 26 September 2023; accepted 9 January 2024; published 1 February 2024)

The numerical approach to calculating the S-matrix poles associated with virtual states in electron-molecule collisions is proposed within the modified effective-range theory frame. The S-matrix continuation into the complex momentum plane is possible thanks to the analytical properties of modified Mathieu functions, that is, the exact solutions of the Schrödinger equation with the long-range polarization potential ($\sim r^{-4}$). The short-range electron-molecule interaction is included in the introduced numerical approach by model comparison with experimental integral, differential, and momentum-transfer elastic cross sections. The influence of the polarization potential on the virtual-state pole positions is analyzed for nonpolar targets such as N_2, CH_4, CO_2, and SF_6. The relation between the S-matrix pole position and the s-wave scattering length is discussed.

DOI: 10.1103/PhysRevA.109.022801

I. INTRODUCTION

Low-energy electron scattering on molecules shows a whole richness of phenomena called "resonances" [1], which manifest as rapid changes of cross sections (total, vibrational excitation [2], dissociative attachment, i.e., formation of fragment negative ions, etc.) in the function of the collision energy. Particularly, polyatomic molecules [3] show many structures in the energy range of a few eV, reflecting their chemical complexity; see, for example, [4]. A prototype for such resonances is the structure observed by Schulz [2] in the vibrational cross section for N_2 at about 2–3 eV (which also manifests as a maximum in the total cross section; see, for example, [5]). Despite decades of studies, theories still find it difficult to predict such resonances' exact positions, amplitudes, and widths.

In general, resonances are related to a significant time delay in the passage of the incident electron wave packet near the target (compared to the transition time in the absence of the resonant interaction). Such a time delay corresponds to the phase change of the incident wave by $\pi/2$ rad above the potential phase shift (i.e., in the absence of the resonance) at the resonant energy. The potential phase shift is present in the scattering process as a slowly changing background for the dynamical resonant interaction. Mathematically, the resonance can also be associated with a pole of the S matrix in the complex momentum plane (k), slightly below the positive real axis by a distance small compared with the distance from the origin [6,7].

A particular case predicted by the theory, where the pole of S matrix lies precisely on the negative imaginary momentum axis, just below the origin is called a virtual state. Unlike typical resonances, the virtual states are not associated with the time delay of an electron wave packet. However, their presence significantly enhances the wave function of the scattered electron near the target due to a strong constructive interference of the incident and reflected waves [8]. Consequently, integral elastic and momentum-transfer cross sections for electron scattering from ground-state molecules increase sharply as the electron energy decreases to zero. This mathematical concept has been used to explain unusually high elastic cross sections at low energies observed for SF_6 [9,10], CO_2 [11,12], and other nonpolar molecules [13,14]. For a long time, the presence of the poles associated with the virtual states had been proven only in semiheuristic ways until the work of Morgan [15], who showed their existence in electron scattering on CO_2 through *ab initio* numerical calculations using the R-matrix method.

Single S-matrix poles associated with virtual states are generally well defined on the negative imaginary axis for the short-range potentials, which disappear beyond a certain distance from the molecule. On the other hand, analytical studies for pure long-range interactions show that the S matrix can have an infinite number of virtual-state poles. Moreover, the S matrix for infinite-range potentials can be plagued with redundant poles and zeros, which do not correspond to any resonance, bound, or virtual state; see [16,17] and references therein.

Electron scattering from molecules comprises both long- and short-range potentials. However, textbooks on quantum mechanics (e.g., see [18]) typically describe virtual states in low-energy electron scattering considering only a finite-range potential. Herzenberg and Saha [8] showed that a true virtual state cannot exist if a long-range dipole potential ($\sim r^{-2}$) is present (i.e., for collisions with polar targets). Such an interaction displaces a pole off the negative imaginary axis to the left on the complex momentum plane. Nevertheless, a displaced pole still profoundly affects low-energy cross sections if the dipole moment is low enough (less than 1.19 D [8]).

[*] kamil@fizyka.umk.pl
[†] karwasz@fizyka.umk.pl

To the best of our knowledge, no studies have been devoted to the effect of long-range polarization potential ($\sim r^{-4}$) on the S-matrix poles associated with the virtual states. Such potential is a dominant long-range interaction in electron scattering by nonpolar molecules due to the dipole induced by the charge of the incoming projectile. Though the R-matrix method intrinsically contains the contribution of this potential; however, the choice of representation of the short-range polarization response of the molecule inside the R-matrix box noticeably affects the S-matrix pole positions [15,19].

In the present paper, we show that the virtual states in electron-molecule collisions can be revealed and studied using Mathieu functions, that is, the analytical solutions for the Schrödinger equation with pure polarization potential (r^{-4}). We follow the conclusions of Khrebtukov [20], who noted that Mathieu functions can be exploited for the S-matrix continuation into the complex momentum plane. The S-matrix poles are examined for SF_6 and CO_2, where virtual states play an important role in electron scattering. For comparison, an identical analysis is performed for N_2 and CH_4, where no unusually significant increase in the elastic cross section towards zero energy is observed. The contribution of the short-range interaction is included in our approach using modified effective-range theory (MERT) [21,22]. More specifically, the contribution of the finite-range potential to the scattering phase shifts is expressed by the parameters of the effective-range expansion, which are determined through model comparison with experimental cross sections. Idziaszek and Karwasz performed MERT analysis for CO_2 and N_2 using only total cross sections [23,24]. In the present paper, for both molecules, we develop the methodology that we proposed previously for CH_4 [25] and SF_6 [26]—the constraints on MERT parameters are imposed simultaneously by integral elastic cross section (IECS), differential cross sections (DCS), and momentum-transfer cross section (MTCS) derived from beam and swarm experiments. Excellent reviews of experimental and theoretical studies on low-energy electron scattering on N_2 and CH_4 can be found in recent work by Song *et al.* [27,28]. For SF_6 and CO_2, please see the recent work [29,30] and references therein.

To reveal the influence of the polarization potential on virtual states, our model, which intrinsically takes into account resonant and nonresonant scattering, is compared with the Feshbach projection-operator formalism introduced by Domcke and coworkers [31–33]. Feshbach's formalism allows studying the poles of the S-matrix resonant part, neglecting the influence of the slowly changing background (as a function of the energy) and long-range interactions. Finally, in light of the present results, we discuss the validity of the relation between the scattering length (A_0) and the S-matrix pole position (k_0) on the complex momentum plane, i.e., $A_0 = i/k_0$. Such a simple relation was used in the past to determine the zero energy cross section in electron-molecule collisions [11,15,19] or the energy of virtual and bound states in positron scattering by atomic and molecular targets [34,35]. Our present results are found to be consistent with the conclusions of the most recent work by Čurík *et al.* [36], which deals with the relation between the scattering length and S-matrix poles.

This paper is organized as follows. In Sec. II, we describe briefly the principles of the modified effective-range theory. Section III includes MERT analysis of elastic integral, differential, and momentum-transfer cross sections for N_2 and CO_2 to parametrize the contribution of the short-range interaction. A similar MERT analysis has already been done for CH_4 and SF_6 in our previous papers [25,26]. Section IV describes the calculations of the S-matrix poles associated with the virtual states using the Feshbach projection-operator formalism and the semianalytical continuation of the S matrix into the complex momentum plane with the help of Mathieu functions. The main conclusions are summarized in Sec. V.

II. MODIFIED EFFECTIVE-RANGE THEORY

The details of the modified effective-range theory have been described in our previous papers [21,22]. Here, we describe it only briefly. The relative motion of the electron and neutral nonpolar molecule can be described by the following radial Schrödinger equation within a partial-wave formalism (in atomic units):

$$\left[\frac{d^2}{dr^2} - \frac{l(l+1)}{r^2} + \left(\frac{e^2\mu}{\hbar^2}\right)\left(\frac{\alpha}{r^4} + V_2(r)\right) + V_s(r) + k^2\right]\Psi_l(r) = 0, \tag{1}$$

where l is the angular momentum quantum number, k is the wave number, α is the dipole polarizability, and $V_s(r)$ is the short-range potential. Since atomic units are employed throughout this paper, the electron mass (m_e), the Planck constant ($\hbar$), and the elementary charge (e) are equal to unity. Consequently, the reduced mass of the electron-molecule system (μ) can be also approximated to 1. Here $V_2(r) = (\alpha_2/r^4 + 2Q/r^3)P_2(\cos\theta)$ denotes the nonisotropic part of the polarization potential with P_2 being the Legendre polynomial of order 2. We further assume that $V_2(r)$ can be neglected compared to α/r^4. This is justified as long as the quadrupole moment Q and the nonspherical polarizability α_2 expressed in atomic units are much smaller than α. As shown in [23] this is an excellent approximation for N_2. For the CO_2 molecule, V_2 is expected to be small at energies below 1 eV as indicated by the results of [24].

MERT was originally developed by O'Malley *et al.* [37], who proposed to include the contribution of the short-range potential $V_s(r)$ in boundary conditions subjected to analytical solutions of the Schrödinger equation with pure long-range polarization potential ($\sim r^{-4}$):

$$\left[\frac{d^2}{dr^2} - \frac{l(l+1)}{r^2} + \left(\frac{e^2\mu}{\hbar^2}\right)\frac{\alpha}{r^4} + k^2\right]\Phi_l(r) = 0. \tag{2}$$

$\Phi_l(r)$ can be expressed in terms of modified Mathieu functions, the behavior of which at small and large distances r is determined by the standard boundary conditions:

$$\Phi_l(r) \overset{r\to 0}{\sim} r\sin\left(\frac{\sqrt{\alpha}}{r} + \gamma_l\right) \quad \text{and} \quad \Phi_l(r) \overset{r\to\infty}{\sim} \sin\left(kr - l\frac{\pi}{2} + \eta_l\right) \tag{3}$$

where γ_l is a parameter determined by the short-range part of the interaction potential, while η_l is the scattering phase shift.

These boundary conditions provide the following expression for the scattering phase shift:

$$\tan\eta_l = \frac{m_l^2 - \tan^2\delta_l + B_l\tan\delta_l\left(m_l^2-1\right)}{\tan\delta_l\left(1-m_l^2\right)+B_l\left(1-m_l^2\tan^2\delta_l\right)}, \tag{4}$$

where $B_l = \tan(\gamma_l + l\pi/2)$ and $\delta_l = \frac{\pi}{2}(\nu_l - l - \frac{1}{2})$. Here m_l and ν_l denote the energy-dependent parameters which can be determined numerically from properties of the Mathieu functions (see the numerical procedures described in [21,22]).

Integral elastic ($\sigma_{\rm IE}$), momentum-transfer ($\sigma_{\rm MT}$) and differential elastic ($d\sigma/d\omega$) cross sections (all measurable directly) are calculated using the standard partial wave expansions:

$$\sigma_{\rm IE} = \frac{4\pi}{k^2}\sum_{l=0}^{\infty}(2l+1)\sin^2\eta_l(k), \tag{5}$$

$$\sigma_{\rm MT} = \frac{4\pi}{k^2}\sum_{l=0}^{\infty}(l+1)\sin^2[\eta_l(k)-\eta_{l+1}(k)], \tag{6}$$

$$\frac{d\sigma}{d\omega} = \frac{1}{k^2}\left|\sum_{l=0}^{\infty}(2l+1)\exp\eta_l\sin\eta_l(k)P_l(\cos\theta)\right|^2 \tag{7}$$

where θ is the scattering angle and $P_l(x)$ are the Legendre polynomials.

O'Malley *et al.* [37] showed that energy dependence of parameter $B_l(k)$, related to the unknown short-range potential, has the following general form:

$$B_l(k) = b_l(0) + \tfrac{1}{2}\sqrt{\alpha e^2\mu/\hbar^2}\rho_l(0,k)k^2. \tag{8}$$

where $b_l(0)$ is the zero energy contribution and

$$\rho_l(0,k) = \int_0^{\infty}\Phi_l(0,r)\Phi_l(k,r) - \Psi_l(0,r)\Psi_l(k,r)dr. \tag{9}$$

Thus far all equations are exact. O'Malley *et al.* [37] proposed to approximate the latter parameter by the energy independent value at zero energy. Then $B_l(k)$ takes the form

$$B_l(k) \approx b_l(0) + \tfrac{1}{2}\sqrt{\alpha e^2\mu/\hbar^2}R_l k^2, \tag{10}$$

where $R_l = \rho_l(0,0)$. Equation 10 is similar to the effective-range expansion of the scattering phase shift in absence of the long-range potentials used to describe neutron-proton collisions [38,39]. Hence, in analogy to the original effective-range theory, we can call R_l the "effective range," though the physical meaning of this parameter is rather different. Since the error is of the order k^4, it is expected that the approximation is valid at low energies. We have already shown [21,22,25,40,41] that $\rho_l(0,k)$ changes rather slowly with increasing energy since MERT (using approximation 10) is able to describe the scattering cross sections almost up to the energy thresholds for the first inelastic processes (i.e., electronic excitation, or positronium formation in case of positron scattering) for many atoms and molecules.

In the zero energy limit both integral elastic [Eq. (5)] and momentum-transfer cross sections [Eq. (6)] can be expressed by the s-wave scattering length (A_0):

$$\sigma_{\rm IE}(k) \approx \sigma_{\rm MT}(k) = 4\pi A_0^2, \quad k\to 0. \tag{11}$$

The s-wave scattering length can be expressed in terms of b_0 as $A_0 = -\sqrt{\alpha e^2\mu/\hbar^2}/b_0$.

At low energies, the leading contributions come mainly from the first two or three partial waves ($l = 0, 1, 2$) while the contributions of higher partial waves are small and they are not modified by the short-range forces due to very high centrifugal barriers associated with large l numbers. Therefore the scattering phase shifts experienced by higher partial waves can be described by Born approximation [37]:

$$\tan\eta_l(k) = \frac{\pi\alpha k^2}{8(l-1/2)(l+1/2)(l+3/2)}. \tag{12}$$

We found that the k^4 terms appearing in phase shifts induced by pure long-range forces (due to charge-induced dipole and quadrupole moments) as presented by Ali and Fraser [42] give only minor correction, so these terms were omitted. In this paper, we consider the contribution of high partial waves up to $l = 12$ using the approximation by Eq. (12).

Substituting Eqs. (4) and (10) for two or three first partial waves [and Eq. (12) for higher partial waves] into Eqs. (5)–(7) one gets relations which can be fitted to experimental data in order to determine the unknown parameters (b_l and R_l) of the effective-range expansion of $B_l(k)$. In this paper, we use experimental values of N_2 and CO_2 dipole polarizabilities, $\alpha = 11.54a_0^3$ and $16.92a_0^3$ [43], respectively. We checked that the MERT fit is weakly dependent on the value of dipole polarizability for both studied molecules, within existing discrepancies of α in the literature.

III. MERT ANALYSIS

A. Molecular nitrogen N_2

To optimize the derivation of MERT coefficients, we have developed a numerical procedure allowing the simultaneous fitting of multiple data sets with shared fitting parameters.

In the present paper, we performed MERT simultaneous fit to integral elastic and momentum-transfer cross sections recommended by Itikawa [45] below 1.5 eV (i.e., below $^2\Pi_g$ shape resonance). We also included differential elastic cross sections by Sun *et al.* [52], which cover a relatively large energy range ($E = 0.55$, 1.0, and 1.5 eV). The DCS data of Sohn *et al.* [53] cover an even more extensive energy range, but as discussed by Song *et al.* [27] these cross sections are probably underestimated due to normalization procedure (unavoidable in cross-beam experiments used for DCS characterization). Figures 1 and 2 show the results of MERT fit. The derived parameters of the effective-range expansion [Eq. (10)] are given in Table I. We found that the phase shifts of three partial waves (s, p, and d) need to be characterized by Eq. (4) to get an agreement between all three datasets. Moreover, the model reproduces DCS by Allan [58] at all scattering angles, including 180°—the angular region inaccessible experimentally for a long time.

Note that the IECS and MTCS recommended by Itikawa [45] are consistent with each other within the frame of the current model except for very low energy (below 10 meV), where MERT-derived MTCS becomes systematically lower than experimental data [see Fig. 1(b)]. However, swarm-derived data below 10 meV recommended by Itikawa represent the effective MTCS defined as the sum of the inelastic CS plus the elastic ones. Recently, Kawaguchi *et al.* [63] noted that

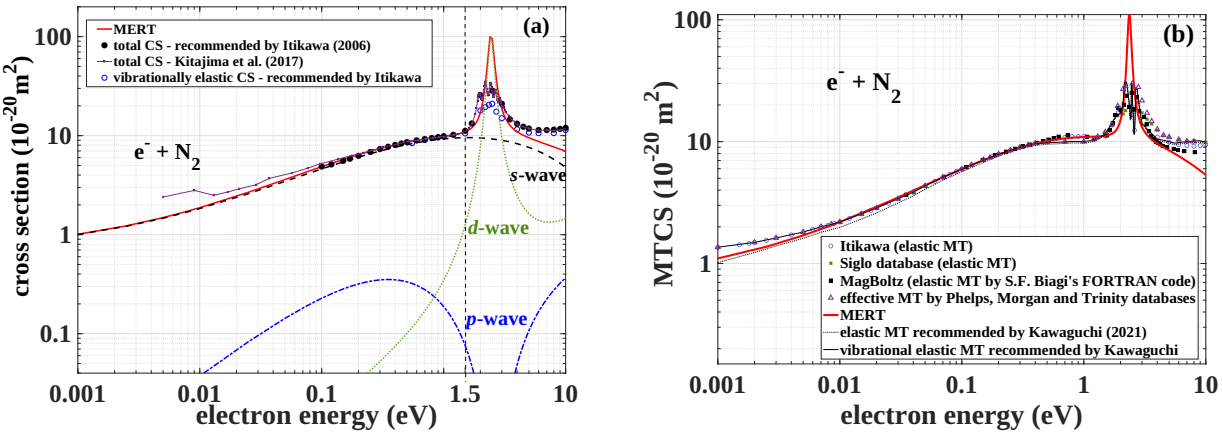

FIG. 1. (a) MERT analysis of integral elastic cross section for electron scattering from molecular nitrogen. Experimental data: Total cross sections (TCS) by Kitajima *et al.* [44] and recommended TCS by Itikawa [45]. The vertical dashed line at 1.5 eV indicates the highest energy used in the fit. MERT-derived partial wave contributions (s, p, and d) to IECS are also shown. (b) MERT-derived momentum-transfer CS compared with swarm-derived data [46–51].

the deexcitation of thermally populated rotational states ($j+2\rightarrow j$) may play a comparable role for pure elastic scattering at very low energies. Using Gerjuoy and Stein's [64] analytical expressions for rotational excitation and deexcitation CS (considering only long-range quadrupole interaction), they decoupled inelastic contribution from the elastic one in the effective MTCS of the IST-LISBON database [51] below 0.3 eV. Our MERT-derived MTCS tends toward their pure elastic data with lowering energy.

Parameters of the MERT fit on such a set of cross sections are given in Table I. Presently derived scattering length $A_0 = 0.435a_0$ is consistent with other determinations, mainly based on the different approaches to the modified effective-range theory. It is interesting to note that A_0 for N_2 is relatively small, positive, and comparable to neon despite a massive difference in dipole polarizability (neon polarizability $\approx 2.6a_0^3$, and scattering length $\approx 0.220a_0$ [69]).

Interestingly, using the fitted parameters, the extension of MERT analysis to higher energies (above 1.5 eV) reveals the resonancelike peak in the IECS and MTCS appearing "spontaneously" in the region of $^2\Pi_g$ resonance. The resonance is purely due to the d wave [see Fig. 1(b)], which undergoes the π phase shift + some smaller energy-dependent (negative) nonresonant phase change [see also the inset in Fig. 5(b)]. This is consistent with the theory of resonances in electron scattering by atoms and molecules described by Schulz [1,70]. A similar "resonancelike" structure was obtained in unconstrained MERT fit to TCS alone in [23]. However, unlike the present paper, the peak appeared in the p wave at higher energies with respect to experimental $^2\Pi_g$ resonance, and the MERT coefficients did not allow for reproducing experimental DCSs at lower energies. In the present analysis, the p- wave contribution reaches a minimum in the resonance region [i.e., the p-wave phase shift changes sign; see Fig. 5(b)]. The "d-wave" character of the shape resonance is consistent with the angular distribution of experimental elastic DCS measured above 1.5 eV (see [71] for detailed discussion). The present model is unable to reproduce resonant experimental elastic DCS due to the strong coupling of elastic and vibrational channels—manifested by the oscillatory variations of IECS as a function of energy in the resonance region ($E >$ 1.5 eV). Nevertheless, it is quite unexpected that it predicates the position of the resonance peak, despite the fact that the effective-range parameters are determined through the comparison with experimental data located energetically below the resonance.

B. Carbon dioxide CO_2

In the present analysis, we performed MERT simultaneous fit to IECS and MTCS recommended by Itikawa [72] and Lozano [29] and DCS by Tanaka *et al.* [82], Gibson [81], and Kochem *et al.* [83] measured below 3 eV (i.e., below $^2\Pi_u$ resonance). We also included in the analysis experimental TCS by Field *et al.* [12] measured below the lowest threshold for

TABLE I. Parameters of the effective-range expansion defined in Eq. (10) for electron scattering from N_2 and the s-wave scattering length (A_0).

	A_0 (a_0)	b_1	b_2	R_0 (a_0)	R_1 (a_0)	R_2 (a_0)
$e^- + N_2$	0.435	−0.540	0.049	−15.755	−0.527	0.069
Fabrikant [65]	0.460	From modified effective-range analysis				
Chang [66]	0.440	From modified effective-range analysis				
Ivanov [67]	0.420	From the energy shifts of the Rydberg states of atoms colliding with N_2				
Morrison [68]	0.420	From body frame modified effective-range analysis				
Idziaszek [21]	0.404	Modified effective-range analysis of total cross sections				

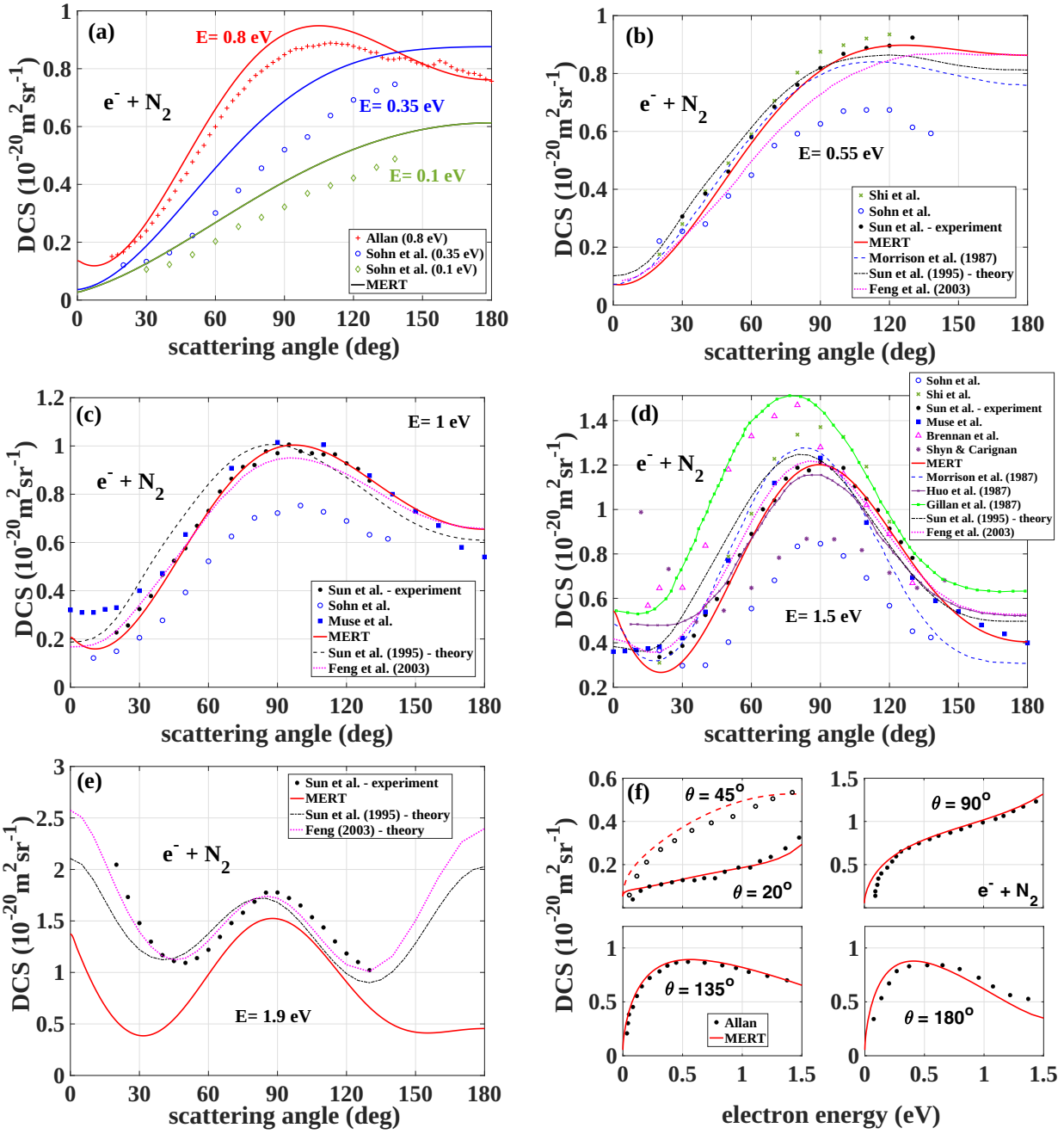

FIG. 2. MERT analysis of differential elastic cross section for electron scattering from molecular nitrogen. DCS vs the scattering angle below the resonance at (a) 0.1, 0.35, and 0.8 eV; (b) 0.55 eV; (c) 1 eV; and (d) 1.5 eV and in the resonance region at (e) 1.9 eV. (f) DCS vs electron energy below 1.5 eV at different scattering angles: 20°, 45°, 90°, 135°, and 180°. Experimental data from Sun *et al.* [52], Sohn *et al.* [53], Muse *et al.* [54], Shi *et al.* [55], Brennan *et al.* [56], Shyn and Carrigan [57], and Allan [58]. Theories by Sun *et al.* [52], Hou *et al.* [59], [60], Morrison *et al.* [61], and Feng *et al.* [62].

vibrational excitation (≈0.08 eV) since it connects smoothly with IECS by Itikawa [72]. Figures 3 and 4 show the results of MERT fit. The derived parameters of the effective-range expansion are given in Table II.

We found that the phase shifts of three partial waves need to be characterized by Eq. (4) to get a relatively good agreement with experiments below the resonance region ($E <$ 3 eV). The extension of MERT analysis to higher energies (above 3 eV) does not reveal any resonancelike peak as it happens for N_2. The partial wave contributions to IECS are shown in Fig. 3(a). Interestingly, the p-wave contribution to IECS reaches the minimum [i.e., the corresponding phase shift changes sign from positive to negative; see Fig. 5(b)] in the proximity of the resonance in a similar way as it happens in N_2. The disappearance of p-wave contribution is responsible for the minimum in the IECS.

Please note, unlike for N_2, the origin of resonance in CO_2 at 3.8 eV is still not fully understood. Herzenberg and Saha's boomerang model [89] suggested the f-wave type of this resonance. On the other hand, Cartwright and Trajmar [88]

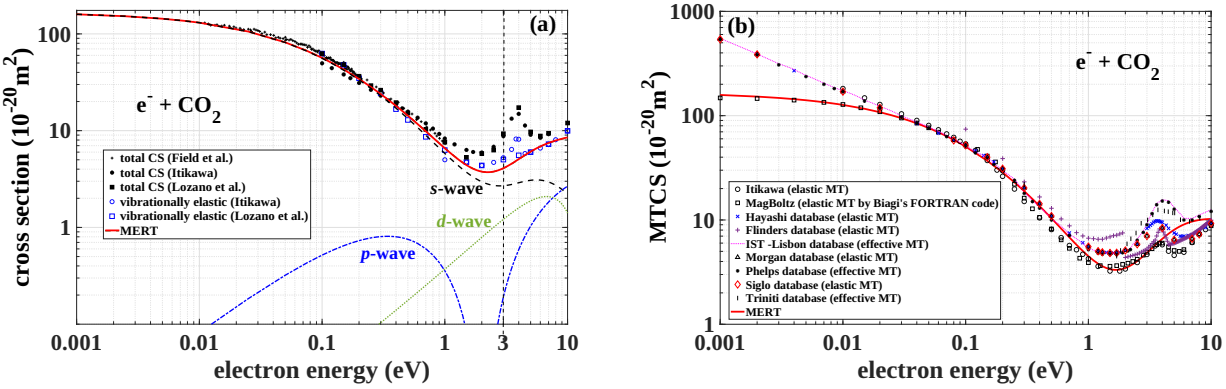

FIG. 3. (a) MERT analysis of integral elastic cross section for electron scattering from carbon dioxide. Experimental data: Total cross sections (TCS) by Field *et al.* [12] and recommended TCS by Itikawa [72] and Lozano *et al.* [29]. The vertical dashed line at 3 eV indicates the highest energy used for the fit. MERT-derived partial wave contributions (s, p, and d) to IECS are also shown. (b) MERT-derived momentum-transfer CS compared with swarm-derived data [73–80].

argued that this peak is a composite structure of shape and Feshbach resonances. Experimental studies [90] of angular distributions of electrons vibrationally (for the 010 bending mode) scattered on CO_2 at 3.8 eV did not indicate a clear (p, d, or f) character of this resonance. Subsequently, Allan [91] discussed the importance of Fermi coupling between different vibrational modes at this resonance. Rescigno *et al.* [92] show that multidimensional treatment of nuclear motion is necessary to describe this resonance with *ab initio* calculations. More recent calculations by Laporta *et al.* [93] indicate measurable progressions of vibrational excitation up to $n' = 10$ for the symmetric stretching mode (and $n' = 2$ for the two other modes); they also show a vibrational-like structure in the elastic channel. Decisively, CO_2 resonance needs further analysis.

We need to underline that the present model cannot reproduce a substantial rise of MTCS below 0.01 eV recommended by many authors. We checked that it is impossible to get

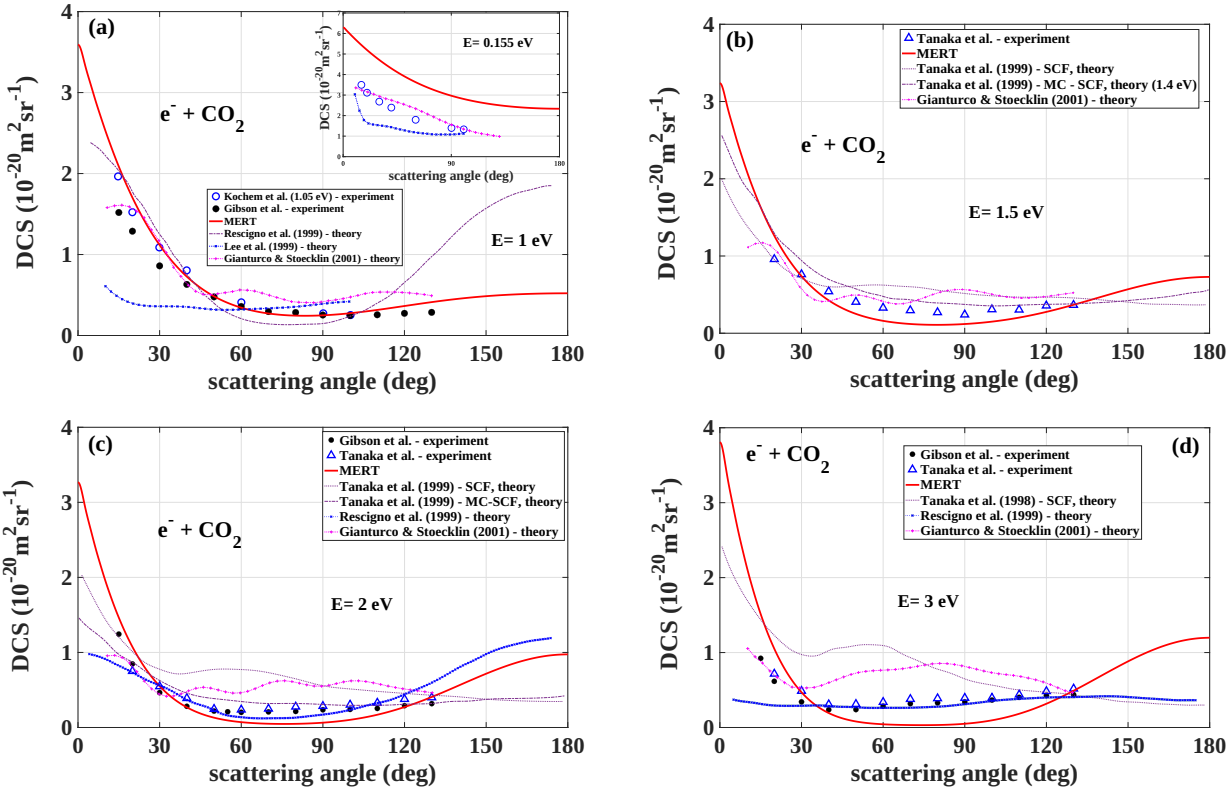

FIG. 4. MERT analysis of differential elastic cross section for electron scattering from carbon dioxide. DCS vs the scattering angle at (a) 1 eV (in the inset at 0.155 eV), (b) 1.5 eV, (c) 2 eV, and (d) 3 eV. Experimental data from Gibson *et al.* [81], Tanaka *et al.* [82], and Kochem *et al.* [83]. Theories by Rescigno *et al.* [84], Lee *et al.* [85], Gianturco and Stoecklin [86], and Tanaka *et al.* [82].

TABLE II. Parameters of the effective-range expansion defined in Eq. (10) for electron scattering from CO_2 and the s-wave scattering length (A_0).

	A_0 (a_0)	b_1	b_2	R_0 (a_0)	R_1 (a_0)	R_2 (a_0)
$e^- + CO_2$ ($s+p$)	−6.95	−0.604	−1.502	−1.382	−0.263	0.622
Singh [87]	−7.20	Semiempirical model fitted to swarm-derived MTCS				
Morrison [11]	−6.17	MERT fit to converged close-coupling calculations				
Fabrikant [65]	−6.8 to −7.2	Modified effective-range analysis				
Estrada [33]	−7.82	Model based on the projection-operator formalism of Feshbach				
Morgan [15]	−4.95	R matrix				
Lee [85]	−4.50	SMC calculations in the SEP approximation				
Idziaszek [24]	−6.60	Modified effective-range analysis of total cross sections				

consistency between this rise and other datasets (regardless of the combination of datasets used in the fitting procedure). Interestingly, MERT agrees with MTCS by Biagi [76] at very low energies, even though this dataset is not included in the fitting.

The present model reproduces very well experimentally determined angular variations of DCS at 1 and 1.5 eV [Figs. 4(a) and 4(b)]. At higher energies [Figs. 4(c) and 4(d)], the experimental DCS becomes nearly constant between 40° and 130° (isotropic scattering). The model has a problem recapturing this feature, and the discrepancy increases with energy. This may be due to the increasing contribution from the anisotropic part of polarization potential and/or phenomena of coupling between the elastic and highly nonpotential vibrational excitations, as observed by Allan [94].

Note also that MERT [see inset of Fig. 4(a)] is much higher than the experimental DCS by Kochem *et al.* [83] measured at a very low energy of 0.155 eV. We checked that it is impossible to integrate these experimental DCSs to get an agreement with experimental TCS [12,72] measured with much lower error at this energy region. Moreover, the declared energy resolution (0.025 eV, which is more than 10% of 0.155 eV) plus the finite angular resolutions of the experimental system plus the expected large transversal extension of the low-energy electron beam suggest that the experimental results at 0.155 eV should be treated with caution.

Presently derived scattering length $A_0 = -6.95a_0$ is consistent with other estimations (see Table II) done using the effective-range analysis of experimental and theoretical data [11,65,87]. Interestingly, all *ab initio*–type calculations such as R-matrix [15] and Schwinger multichannel method in static-exchange-polarization (SMC-SEP) approximation [85] predict much lower values (though consistent with each other). This reflects that R-matrix and SMC-SEP methods give significantly lower IECS than experiments below 1 eV. Consequently, some semiempirical corrections of polarization response are necessary to increase theoretical cross sections at low energies [19].

C. Phase-shift analysis

In Fig. 5, we show MERT-derived phase shifts of partial waves for N_2 and CO_2. Notice that the s-wave phase shift (η_0) for CO_2 is in perfect agreement with close-coupling calculations by Morrison [11]. Compared with the current results, we also present the phase shifts determined in our previous works for CH_4 [40] and SF_6 [26]. It is necessary to mention that the MERT analysis was performed for the latter molecule, considering the coupling of the elastic channel with strong electron attachment in the low-energy range (treated as the absorptive process). The MERT-derived s-wave phase shift for SF_6 remains in perfect agreement with the calculations of Fabrikant *et al.* [10].

The s-wave phase shift changes from purely negative for N_2 (repulsive interaction) to purely positive for CO_2 and SF_6 (attractive interaction) at energies below 1 eV. The CH_4 lies in

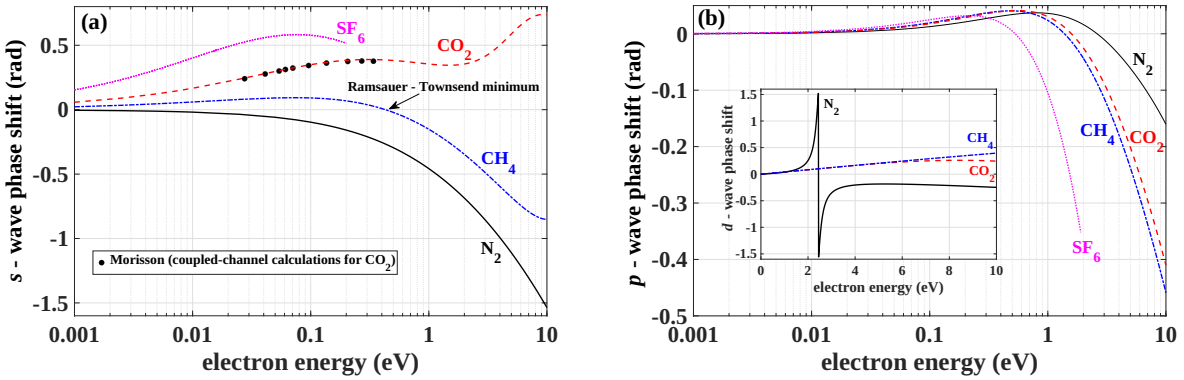

FIG. 5. MERT-derived partial wave scattering phase shifts for N_2, CO_2 (present results), CH_4 [25], and SF_6 [26]: (a) s-wave phase shift (the coupled-channel calculations of s-wave phase shift for CO_2 by Morrison [11] are also presented) and (b) p-wave phase shift. The inset shows d-wave phase shifts.

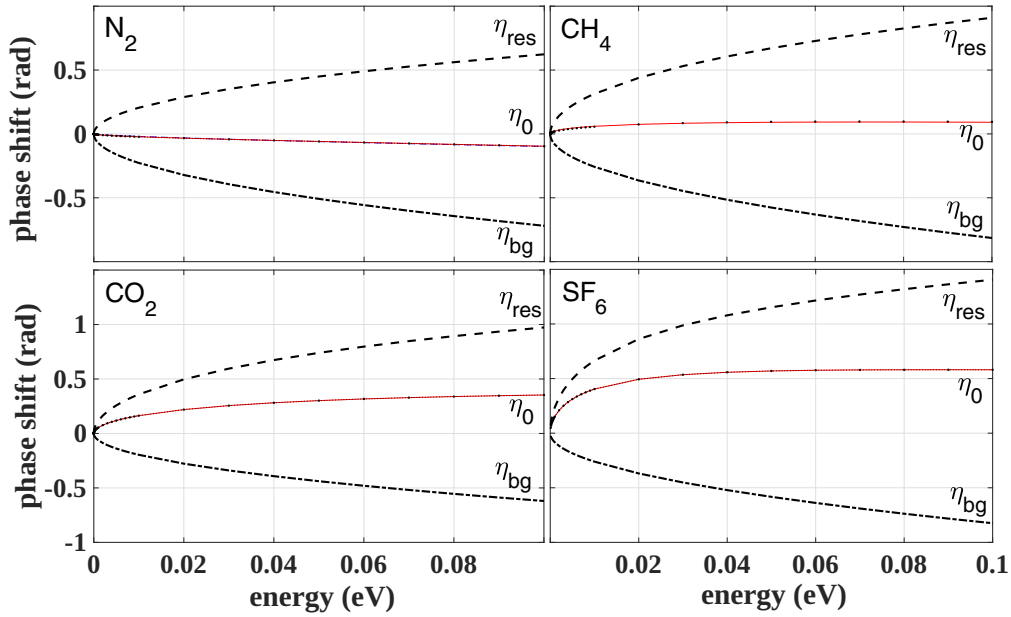

FIG. 6. Feshbach projection-operator formalism fit to MERT-derived s-wave phase shift (η_0) below 0.1 eV for N_2, CH_4, CO_2, and SF_6. The decomposition of the phase shift into a positive resonant term (η_{res}, dashed line) and a negative background term (η_{bg}, dash-dotted line) is also shown.

between since the s-wave phase shift changes the sign at the energy ($\approx$0.5 eV) corresponding to the Ramsauer-Townsend minimum in the IECS. The overall character of η_0 energy dependence is rather weakly related to the polarization of the molecule since CO_2 and CH_4 have almost identical static dipole polarizabilities (α). On the other hand, the strength of polarization interaction is visible in the p-wave phase shifts (η_1) since stronger polarizability corresponds to lower energy where the sign change of η_1 occurs.

Strong, attractive interaction in low-energy electron scattering by CO_2 and SF_6 translates to a marked rise of IECS toward zero energy. This behavior is explained by the existence of a pole in the S matrix on the negative imaginary momentum (k) axis near the origin. Estrada and Domcke [33] developed a Feshbach projection-operator formalism to estimate the pole's location from the s-wave scattering phase shift (η_0). However, this model does not include the effect of the long-range polarization potential ($\sim r^{-4}$). On the other hand, the numerical calculations of parameters appearing in the Mathieu functions [i.e., δ_l and m_l in Eq. (4)] for complex k can be used to find S-matrix poles as suggested by Khrebtukov [20]. In the subsequent section, we compare the prediction of Estrada and Domcke's approach with the results obtained by the direct continuation of the S matrix into the imaginary k plane using analytical solutions of the Schrödinger equation for the r^{-4} potential.

IV. S-MATRIX POLES

A. Virtual states by Feshbach projection-operator formalism

In the Feshbach projection-operator formalism [33], the scattering phase shift is decomposed into the background and resonant terms:

$$\eta_0 = \eta_{bg} + \eta_{res}. \tag{13}$$

The unknown background contribution is approximated by the leading term of its threshold expansion,

$$\eta_{bg} = 2^{-1/2}\zeta k, \tag{14}$$

while the resonant part is given by the following expression:

$$\eta_{res} = -\tan^{-1}\left(\frac{2^{-1/2}\xi k \exp(-k^2/2\chi)}{k^2/2 - \epsilon_d - \mathrm{Re}[F(k)]}\right). \tag{15}$$

Here

$$F(k) = -\frac{1}{2}\xi\left[\left(\frac{\pi}{\chi}\right)^{-1/2} + i2^{-1/2}k\,w\left(\frac{k}{\sqrt{2\chi}}\right)\right], \tag{16}$$

where $w(z)$ is a Faddeeva function. The unknown parameters ζ, ξ, ϵ_d, and χ can be determined numerically by fitting the model to s-wave scattering phase shifts at low energies. In Fig. 6, we present such fits to the MERT-derived η_0 below 0.1 eV for all four considered molecules. The decomposition of phase shift into the resonant and nonresonant parts is also shown. Notice that the negative background contribution is comparable in magnitude to the positive resonant term. The slight imbalance between both terms determines the overall nature of the scattering. In particular, the nonresonant scattering dominates for N_2 in the considered energy range, while the opposite occurs for other molecules.

The poles of the resonant S matrix corresponding to η_{res} are given by the complex solutions of

$$\tfrac{1}{2}k^2 - \epsilon_d - F(k) = 0. \tag{17}$$

Since $F(k)$ is real valued on the imaginary k axis, Eq. (17) can be solved graphically. The solutions are shown in Fig. 7 using energy as a variable. The broken line represents $F(k)$ for $ik < 0$, while the dotted curve corresponds to $F(k)$ for $ik > 0$ (and its real part on the positive real k axis, i.e., for $E > 0$). As expected, the pole position (k_0) lies the closest to the origin

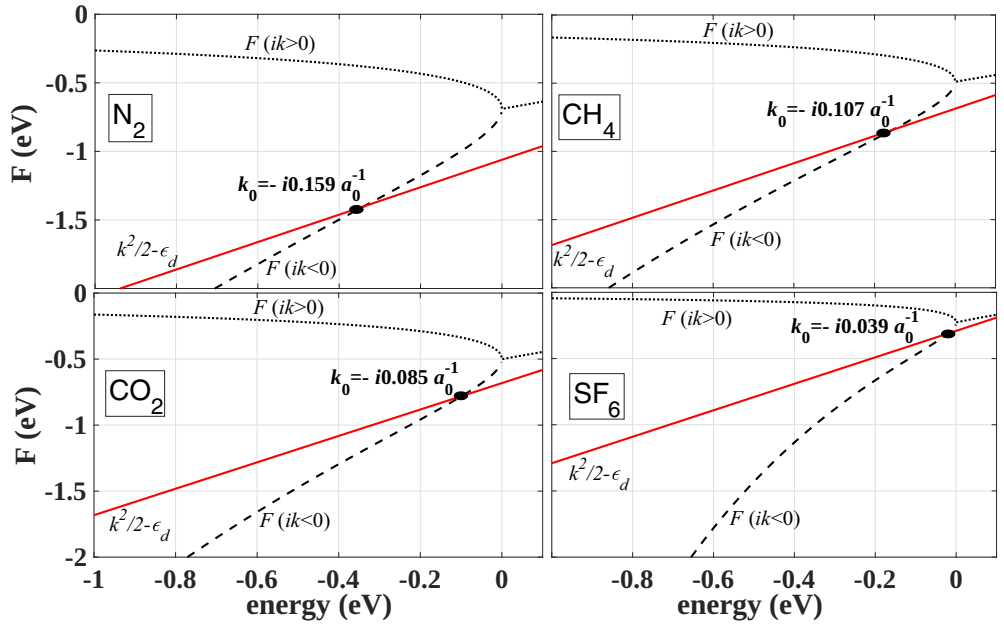

FIG. 7. Graphical determination of the resonant S-matrix pole position (k_0) in the Feshbach projection-operator formalism—the solution of Eq. (17). The dashed and dotted curves represent the $F(k)$ function for $ik < 0$ and $ik > 0$, respectively. The black dot indicates the $k^2/2 - \epsilon_d$ intersection with $F(k)$ function.

of the complex momentum plane for SF_6 and CO_2, while it departs away from the origin for CH_4 and N_2. Notably, the presently derived k_0 for CO_2 is much lower than the value reported in [33], the authors of which carried out precisely the same analysis for this molecule. We checked carefully that the numerical values of model parameters provided by Estrada and Domcke [33] cannot give the pole position reported by these authors, but rather the value very close to the one derived in the present paper.

B. Semianalytical continuation of the S matrix using modified Mathieu functions

O'Malley *et al.* [37] pointed out that Mathieu functions are valid not only for real and positive k but rather in the sector $-\pi < \text{Arg } k < \pi$. Khrebtukov [20] used this property to estimate the positions of resonances (i.e., the S-matrix poles) in electron scattering from alkali-metal atoms. We benefit from this feature to continue the S matrix defined for real k as

$$S_l(k) = e^{2i\eta_l(k)}, \tag{18}$$

into the complex momentum plane. This is done by calculating η_l using Eq. (4) with MERT-derived parameters of the effective-range expansion along with δ_l, m_l, and B_l computed for complex k. The pole in the S matrix formally corresponds to the condition $\tan \eta_l = -i$.

We checked that the S matrix calculated in such a way fulfills the unitary condition $S_l(k)S_l^*(k^*) = 1$ [6,7] for any complex value of k. This implies that η_l is real when k is real. Note that, unlike the Feshbach formalism, this approach considers intrinsically the contribution of resonant and nonresonant interactions in the presence of long-range polarization potential.

First, we checked whether the d-wave resonance in the electron scattering from the N_2 molecule [see Fig. 1(b) and the inset of Fig. 5(b)] is reflected in the S matrix plotted on the complex momentum plane. We easily found the pole of S_2 just below the real axis at $k = 0.42a_0^{-1}$ (i.e., $E = 2.4$ eV) where the maximum of shape resonance is present. This result confirmed that the proposed approach allows for determining the matrix poles corresponding to the real effects in the scattering process.

Since a virtual-state interaction occurs at very low energies, we consider only the s-wave scattering in further analysis. We found, without difficulty, poles of S_0 in the lower half of the complex momentum plane for all four considered molecules; see Fig. 8. The poles are displaced from the negative imaginary k axis to the left, so they do not represent true virtual states (as it is defined for finite-range potentials). This shows that a polarization potential (r^{-4}) affects the poles' positions similarly to a long-range dipole potential (r^{-2}) in polar molecules [8]. Since the poles are off the imaginary axis, one would expect a pair of poles located symmetrically relative to this axis. However, since the long-range potentials, such as r^{-4}, cause a branch point at $k = 0$ [31], the mirror image of the pole is located on a different Riemann sheet. This sheet can be found by the proper S-matrix rotation around the origin [95].

The S-matrix pole positions determined in the present approach are compared with Feshbach projection-operator formalism in Table III. As expected, the pole position for SF_6 is closest to the origin. Moreover, Feshbach's and Mathieu's approaches predict the same pole positions along the imaginary axis for this molecule. This suggests that the resonant terms of the S matrix dominate strongly over nonresonant ones. Consequently, the pole position along the imaginary axis does not shift between methods despite the matrix's analytic

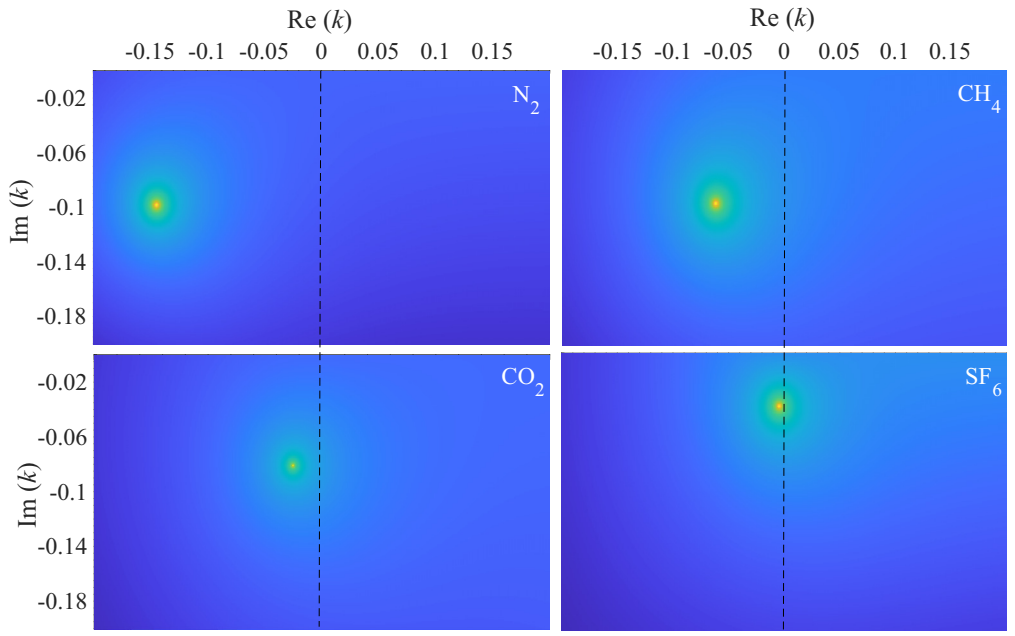

FIG. 8. Poles in the $|S_0|$ matrix on the complex momentum plane (k in a_0^{-1} units) calculated with a semianalytical approach based on modified Mathieu functions.

structure change caused by the polarization potential included in Mathieu's approach (moving the poles off the axis). The poles depart further from the origin for CO_2, CH_4, and N_2, respectively. Moreover, the discrepancies between Feshbach's and Mathieu's methods regarding the pole position along the imaginary axis also increase in this order. This is due to the progressive weakening of resonant scattering with respect to the background interaction. This suggests that the approximation for nonresonant phase shift proposed in the Feshbach method, i.e., Eq. (14), is not sufficiently strong to describe this contribution for CO_2, CH_4, and N_2.

Notice that the presently determined pole position along the imaginary axis for CO_2, i.e., $-0.081i\ a_0^{-1}$, is lower in absolute magnitude than the previous determination by R-matrix calculations, $-0.20i\ a_0^{-1}$ [15] and $-0.14i\ a_0^{-1}$ [19], as well as the semiempirical method by Morrison, $-0.1620i\ a_0^{-1}$ [11]. None of these works observed a pole position shift off the imaginary axis for the $^2\Sigma_g^+$ molecular symmetry (i.e., at equilibrium geometry when no permanent dipole moment is present). Importantly, the pole positions from works [11,15,19] were used to estimate the scattering length assuming $A_0 = i/k_0$ (see also Table II). However, as noted recently by Čurík *et al.* [36], such a simple relation between A_0 and k_0 neglects the background phase contribution. This last work proved that the unknown nonresonant phase could not be ruled out considering spherically symmetric short-range potentials. We expect that a similar conclusion remains valid in the presence of long-range interactions. Our comparison of Feshbach's and Mathieu's approaches for predicting the S-matrix pole position confirms the importance of background scattering.

We need to comment briefly on the S-matrix pole position for CO_2 determined by Morrison [11]. This location was determined by extrapolating the close-coupled calculations of $\eta_o(k)$ at low energies [see also Fig. 5(a)] towards the zero energy point ($k = 0$) using the power series expansion of the expression $k \cot \eta_0(k) = -k_0 + \rho k^2/2$. This is an effective-range expansion of the scattering phase shift around the pole position ($k = k_0$) derived by O'Malley *et al.* [37]. Due to the absence of the linear term in k, this expansion can be used as long as the linear term in $\eta_o(k)$ can be neglected in the neighborhood of $k = 0$ (see the discussion in [37]). However, MERT-derived η_0 for CO_2 in the present paper shows that the term in k dominates the term in k^2 over a relatively wide energy range. Hence, it cannot be neglected when analyzing scattering phase shift at low energies, and the quadratic expansion of $k \cot \eta_0(k)$ is inappropriate.

Finally, in Fig. 9, we present the structure of the S-matrix pole related to electron scattering from CO_2. The real and imaginary parts of S_0 undergo abrupt changes from negative to positive values around the pole position. Moreover, peak-valley structures of real and imaginary parts are slightly shifted with respect to each other, resulting in a smooth

TABLE III. The S-matrix pole positions on the complex momentum plane (k in a_0^{-1} units).

	N_2	CH_4	CO_2	SF_6
Feshbach formalism	$0.000 - i0.159$	$0.000 - i0.107$	$0.000 - i0.085$	$0.000 - i0.039$
Mathieu functions	$-0.144 - i0.098$	$-0.061 - i0.097$	$-0.025 - i0.081$	$-0.005 - i0.039$

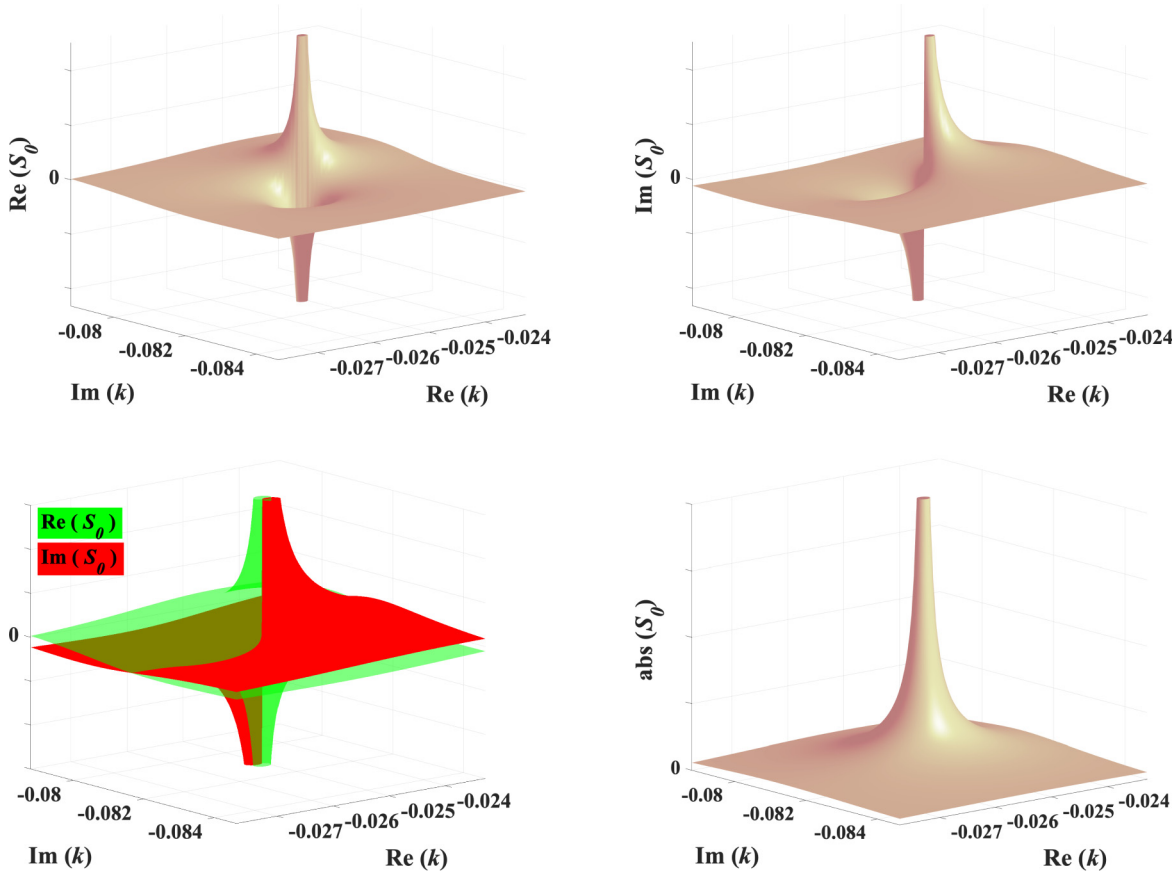

FIG. 9. The structure of a virtual-state S-matrix pole for electron scattering from CO_2: (a) real part of S_0, (b) imaginary part of S_0, (c) overlap of Re(S_0) and Im(S_0), and (d) absolute value of S_0. Identical structures were found for other studied molecules.

(almost symmetrical) peak in the absolute value. We found that the poles for other studied molecules have the same structure.

V. CONCLUSIONS

In this paper, we showed that analytical solutions of the Schrödinger equation with a long-range polarization potential ($\sim r^{-4}$) expressed in terms of modified Mathieu functions can be used for the S-matrix continuation into the complex momentum plane. In particular, the virtual states in the low-energy electron scattering by nonpolar molecules such as N_2, CO_2, CH_4, and $SF4_6$ can be identified. The contribution of short-range interaction between the projectile and the target is parametrized by the coefficients of the effective-range expansion defined within the frame of the modified effective-range theory. The latter are estimated by comparing carefully the model with experimental cross sections (integral, differential, and momentum transfer). In the present paper, we applied this methodology, used previously for CH_4 [25] and SF_6 [26], to N_2 and CO_2. The MERT parameters were derived from integral, differential, and momentum-transfer elastic cross sections.

Interestingly, for the N_2 molecule, it turned out that the obtained MERT parametrization derived at low energies predicts the d-wave resonance exactly at the position of the $^2\Pi_g$ experimental peak. This was confirmed by the pole of the S matrix in the complex k plane appearing just below the real axis at the resonant energy.

The virtual-state poles were found to be displaced off the negative imaginary axis to the left on the complex momentum plane for all studied molecules. Hence, the polarization potential (r^{-4}) has the same effect on the position of the poles as the dipole potential (r^{-2}). Nevertheless, poles for SF_6 and CO_2 are still close enough to the axis to significantly enhance the elastic cross section in the low-energy range.

A comparison of the present approach with the Feshbach projection-operator formalism showed that the competition between resonant and nonresonant scattering determines the amount of the virtual-state pole displacement. The background contribution must be addressed if one wants a complete picture of the scattering process (especially in the presence of long-range forces). In particular, the scattering length (A_0) cannot be estimated from the position of the virtual-state pole (k_0) on the negative imaginary axis (i.e., using simply $A_0 = i/k_0$) without including the nonresonant contribution, which was quite a common practice until now. This finding confirms the conclusions of the recent studies [36] on the relation between the scattering length and S-matrix poles.

[1] G. J. Schulz, Rev. Mod. Phys. **45**, 423 (1973).
[2] G. J. Schulz, Phys. Rev. **125**, 229 (1962).
[3] G. P. Karwasz, R. S. Brusa, and A. Zecca, La Rivista del Nuovo Cimento **24**, 1 (2001).
[4] P. Możejko, G. Kasperski, C. Szmytkowski, A. Zecca, G. Karwasz, L. Del Longo, R. Brusa, and A. Zecca, Eur. Phys. J. D **6**, 481 (1999).
[5] A. Zecca, G. P. Karwasz, and R. S. Brusa, La Rivista del Nuovo Cimento **19**, 1 (1996).
[6] R. G. Newton, *Scattering Theory of Waves and Particles* (Springer-Verlag, Berlin, 1982), Chap. 12, p. 331.
[7] P. G. Burke and C. J. Joachain, *The Theory of Electron-Atom Collisions, Part 1: Potential Scattering* (Springer, New York, 1995), Chap. 3, p. 103.
[8] A. Herzenberg and B. C. Saha, J. Phys. B **16**, 591 (1983).
[9] D. Field, N. C. Jones, and J.-P. Ziesel, Phys. Rev. A **69**, 052716 (2004).
[10] I. I. Fabrikant, H. Hotop, and M. Allan, Phys. Rev. A **71**, 022712 (2005).
[11] M. A. Morrison, Phys. Rev. A **25**, 1445 (1982).
[12] D. Field, N. C. Jones, S. L. Lunt, and J.-P. Ziesel, Phys. Rev. A **64**, 022708 (2001).
[13] A. Souza Barbosa and M. H. F. Bettega, J. Chem. Phys. **146**, 154302 (2017).
[14] L. V. S. Dalagnol, G. M. Moreira, A. Souza Barbosa, and M. H. F. Bettega, J. Phys. Chem. A **127**, 6486 (2023).
[15] L. A. Morgan, Phys. Rev. Lett. **80**, 1873 (1998).
[16] A. Moroz and A. E. Miroshnichenko, New J. Phys. **21**, 103035 (2019).
[17] M. Gadella, A. Hernandez-Ortega, S. Kuru, and J. Negro, Eur. Phys. J. Plus **135**, 822 (2020).
[18] L. D. Landau and L. M. Lifshitz, *Quantum Mechanics: Non-Relativistic Theory* (Pergamon, New York, 1965), Chap. XVII, p. 505.
[19] S. Mazevet, M. A. Morrison, L. A. Morgan, and R. K. Nesbet, Phys. Rev. A **64**, 040701(R) (2001).
[20] D. B. Khrebtukov, J. Phys. A **26**, 6357 (1993).
[21] Z. Idziaszek and G. Karwasz, Phys. Rev. A **73**, 064701 (2006).
[22] K. Fedus, G. P. Karwasz, and Z. Idziaszek, Phys. Rev. A **88**, 012704 (2013).
[23] Z. Idziaszek and G. Karwasz, Eur. Phys. J. D **51**, 347 (2009).
[24] Z. Idziaszek and G. Karwasz, arXiv:0708.2991.
[25] K. Fedus and G. Karwasz, Eur. Phys. J. D **68**, 93 (2014).
[26] K. Fedus, Eur. Phys. J. D **76**, 55 (2022).
[27] M.-Y. Song, H. Cho, G. P. Karwasz, V. Kokoouline, and J. Tennyson, J. Phys. Chem. Ref. Data **52**, 023104 (2023).
[28] M.-Y. Song, J.-S. Yoon, H. Cho, Y. ICkawa, G. P. Karwasz, V. Kokoouline, Y. Nakamura, and J. Tennyson, J. Phys. Chem. Ref. Data **44**, 023101 (2015).
[29] A. I. Lozano, A. García-Abenza, F. Blanco R., M. Hasan, D. S. Slaughter, T. Weber, R. P. McEachran, R. D. White, M. J. Brunger, P. Limão-Vieira, and G. García Gómez-Tejedor, J. Phys. Chem. A **126**, 6032 (2022).
[30] B. Goswami and B. Antony, RSC Adv. **4**, 30953 (2014).
[31] W. Domcke, J. Phys. B **14**, 4889 (1981).
[32] W. Domcke and L. S. Cederbaum, J. Phys. B **14**, 149 (1981).
[33] H. Estrada and W. Domcke, J. Phys. B **18**, 4469 (1985).
[34] C. M. Surko, G. F. Gribakin, and S. J. Buckman, J. Phys. B **38**, R57 (2005).
[35] G. F. Gribakin, J. A. Young, and C. M. Surko, Rev. Mod. Phys. **82**, 2557 (2010).
[36] R. Čurík, M. Tarana, and J. C. V. Horáček, Phys. Rev. A **108**, 012807 (2023).
[37] T. F. O'Malley, L. Spruch, and L. Rosenberg, J. Math. Phys. **2**, 491 (1961).
[38] H. A. Bethe, Phys. Rev. **76**, 38 (1949).
[39] J. M. Blatt and J. D. Jackson, Phys. Rev. **76**, 18 (1949).
[40] K. Fedus, Phys. Scr. **89**, 105401 (2014).
[41] K. Fedus and G. P. Karwasz, Eur. Phys. J. D **75**, 76 (2021).
[42] M. K. Ali and P. A. Fraser, J. Phys. B **10**, 3091 (1977).
[43] T. N. Olney, N. Cann, G. Cooper, and C. Brion, Chem. Phys. **223**, 59 (1997).
[44] M. Kitajima, T. Kishino, T. Okumura, N. Kobayashi, A. Sayama, Y. Mori, K. Hosaka, T. Odagiri, M. Hoshino, and H. Tanaka, Eur. Phys. J. D **71**, 139 (2017).
[45] Y. Itikawa, J. Phys. Chem. Ref. Data **35**, 31 (2006).
[46] N_2 on SIGLO database, http://lxcat.net, accessed 2023-07-30.
[47] N_2 on Phelps database, http://lxcat.net, accessed 2023-07-30.
[48] N_2 on Morgan database, http://lxcat.net, accessed 2023-07-30.
[49] N_2 on Biagi database, http://lxcat.net, accessed 2023-07-30.
[50] N_2 on TRINITI database, http://lxcat.net, accessed 2023-07-30.
[51] N_2 on IST-Lisbon database, http://lxcat.net, accessed 2023-07-30.
[52] W. Sun, M. A. Morrison, W. A. Isaacs, W. K. Trail, D. T. Alle, R. J. Gulley, M. J. Brennan, and S. J. Buckman, Phys. Rev. A **52**, 1229 (1995).
[53] W. Sohn, K. H. Kochem, K. M. Scheuerlein, K. Jung, and H. Ehrhardt, J. Phys. B **19**, 4017 (1986).
[54] J. Muse, H. Silva, M. C. A. Lopes, and M. A. Khakoo, J. Phys. B **41**, 095203 (2008).
[55] X. Shi, T. M. Stephen, and P. D. Burrow, J. Phys. B **26**, 121 (1993).
[56] M. J. Brennan, D. T. Alle, P. Euripides, S. J. Buckman, and M. J. Brunger, J. Phys. B **25**, 2669 (1992).
[57] T. W. Shyn and G. R. Carignan, Phys. Rev. A **22**, 923 (1980).
[58] M. Allan, J. Phys. B **38**, 3655 (2005).
[59] W. M. Huo, T. L. Gibson, M. A. P. Lima, and V. McKoy, Phys. Rev. A **36**, 1632 (1987).
[60] C. J. Gillan, C. J. Noble, and P. G. Burke, J. Phys. B **21**, L53 (1988).
[61] M. A. Morrison, B. C. Saha, and T. L. Gibson, Phys. Rev. A **36**, 3682 (1987).
[62] H. Feng, W. Sun, and M. A. Morrison, Phys. Rev. A **68**, 062709 (2003).
[63] S. Kawaguchi, K. Takahashi, and K. Satoh, Plasma Sources Sci. Technol. **30**, 035010 (2021).
[64] E. Gerjuoy and S. Stein, Phys. Rev. **97**, 1671 (1955).
[65] I. I. Fabrikant, J. Phys. B **17**, 4223 (1984).
[66] E. S. Chang, J. Phys. B **14**, 893 (1981).
[67] G. K. Ivanov, Calculation of the spectral characteristics of a highly excited atom in a foreign gas, Opt. Spektrosk. **40**, 965 (1976).
[68] M. A. Morrison, W. Sun, W. A. Isaacs, and W. K. Trail, Phys. Rev. A **55**, 2786 (1997).
[69] Y. Cheng, L. Y. Tang, J. Mitroy, and M. S. Safronova, Phys. Rev. A **89**, 012701 (2014).
[70] G. J. Schulz, Rev. Mod. Phys. **45**, 378 (1973).
[71] S. J. Buckman, D. T. Alle, M. J. Brennan, P. D. Burrow, J. C. Gibson, R. J. Gulley, M. Jacka, D. S. Newman, A. R. P. Rau,

J. P. Sullivan, and K. W. Trantham, Aust. J. Phys. **52**, 473 (1999).
[72] Y. Itikawa, J. Phys. Chem. Ref. Data **31**, 749 (2002).
[73] CO_2 on SIGLO database, http://lxcat.net, accessed 2023-07-30.
[74] CO_2 on Phelps database, http://lxcat.net, accessed 2023-07-30.
[75] CO_2 on Morgan database, http://lxcat.net, accessed 2023-07-30.
[76] CO_2 on Biagi database, http://lxcat.net, accessed 2023-07-30.
[77] CO_2 on TRINITI database, http://lxcat.net, accessed 2023-07-30.
[78] M. Grofulović, L. L. Alves, and V. Guerra, J. Phys. D **49**, 395207 (2016).
[79] CO_2 on Flinders database, http://lxcat.net, accessed 2023-07-30.
[80] CO_2 on Hayashi database, http://lxcat.net, accessed 2023-07-30.
[81] J. C. Gibson, M. A. Green, K. W. Trantham, S. J. Buckman, P. J. O. Teubner, and M. J. Brunger, J. Phys. B **32**, 213 (1999).
[82] H. Tanaka, T. Ishikawa, T. Masai, T. Sagara, L. Boesten, M. Takekawa, Y. Itikawa, and M. Kimura, Phys. Rev. A **57**, 1798 (1998).
[83] K. H. Kochem, W. Sohn, N. Hebel, K. Jung, and H. Ehrhardt, J. Phys. B **18**, 4455 (1985).
[84] T. N. Rescigno, D. A. Byrum, W. A. Isaacs, and C. W. McCurdy, Phys. Rev. A **60**, 2186 (1999).
[85] C.-H. Lee, C. Winstead, and V. McKoy, J. Chem. Phys. **111**, 5056 (1999).
[86] F. A. Gianturco and T. Stoecklin, J. Phys. B **34**, 1695 (2001).
[87] Y. Singh, J. Phys. B **3**, 1222 (1970).
[88] D. C. Cartwright and S. Trajmar, J. Phys. B **29**, 1549 (1996).
[89] C. Szmytkowski and M. Zubek, J. Phys. B-At Mol. Opt. **10**, L31 (1977).
[90] T. Antoni, K. Jung, H. Ehrhardt, and E. S. Chang, J. Phys. B **19**, 1377 (1986).
[91] M. Allan, Phys. Rev. Lett. **87**, 033201 (2001).
[92] T. N. Rescigno, W. A. Isaacs, A. E. Orel, H.-D. Meyer, and C. W. McCurdy, Phys. Rev. A **65**, 032716 (2002).
[93] V. Laporta, J. Tennyson, and R. Celiberto, Plasma Sources Sci. Technol. **25**, 06LT02 (2016).
[94] M. Allan, J. Phys. B **35**, L387 (2002).
[95] A. Herzenberg, J. Phys. B **17**, 4213 (1984).